

Adalbert Feltz

Amorphous Inorganic Materials and Glasses

© VCH Verlagsgesellschaft mbH, D-6940 Weinheim (Federal Republic of Germany), 1993

Distribution:
VCH, P.O. Box 10 11 61, D-6940 Weinheim (Federal Republic of Germany)
Switzerland: VCH, P. O. Box, CH-4020 Basel (Switzerland)
United Kingdom and Ireland: VCH (UK) Ltd., 8 Wellington Court,
Cambridge CB1 1HZ (England)
USA and Canada: VCH, 220 East 23rd Street, New York, NY 10010-4606 (USA)

ISBN 3-527-28421-4 (VCH, Weinheim)

ISBN 1-56081-212-5 (VCH, New York)



Weinheim · New York
Basel · Cambridge · Tokyo

coherent films, wires, or fibres with macroscopic dimensions in at least one or two directions. In both cases an essential feature of these materials is that they have a transition temperature region.

Glasses have numerous properties in common with crystalline solids, such as hardness and elasticity of shape.

In the history of glass-making for the most diverse uses, extending over more than four thousand years, high-temperature methods of melting mixtures of inorganic substances with subsequent solidification to glass in a cooling process have worked extremely well. That is why the definitions of the glass state emphasize its origin from the melt. The following formulation [2.1] of 1971 refers to the definition given by the American Society of Testing Materials:

"Glass is an inorganic product of melting, solidified mainly without crystallization."

The large group of organic glasses, many of which also have important technical applications, truly have the nature of vitreous solids. In addition, it should be stressed that research in the past two decades has led to many new preparative methods, by which amorphous and, at the same time, vitreous states of elements and compounds can be achieved without melting. This has greatly extended the variety of such states that can be prepared, and has stimulated efforts towards increased understanding in this field.

Thin amorphous or vitreous layers in particular have been intensively studied in this context. It is found that differences from compact glasses are often of degree rather than fundamental in, so that a strict distinction between amorphous layers and compact glasses is not justified at all.

In this book, we follow the opinion expressed in many recent papers that amorphous substances, irrespective of the method of preparation, ought to be defined as vitreous

if they have a transition temperature region, the property typical of glasses.

Also earlier literature used the terms "amorphous" and "vitreous" interchangeably to describe, for example, certain modifications of phosphorus, arsenic, and selenium. This is not contradictory to the conclusion that the term "amorphous solid state" has a more comprehensive meaning, broader than that of the "vitreous state". All glasses are amorphous, but not all amorphous substances are glasses. Highly disperse powders, such as many precipitation products from aqueous solutions, including certain hydroxides, sulphides, and selenides, or intermediate products resulting from certain reactions with solids, as well as thermally unstable gels, can be amorphous, but must not be understood as glasses.

The world of quasicrystalline solids occupies a position between the crystalline and amorphous states of matter. These materials seem to represent a fundamentally new phase of solid matter, exhibiting symmetries that are impossible for ordinary crystals [1.48]. After Penrose [2.516] in 1974 introduced the concept of the two-dimensional quasiperiodic pattern, consisting of two rhombi with fivefold rotational symmetry, octagonal and decagonal quasicrystalline patterns were constructed by computation (for reviews see [1.48, 2.517, 3.861]). The structures obey the deflation rules of self-similarity. They are not simply nonperiodic. Instead, the tiling has a well-defined long-range orientational order over noncrystallographic symmetry operations. However, translational long-range order is absent. Instead there is a quasiperiodicity, leading to a well-defined X-ray diffraction pattern. Shechtman, Blech, Gratias and Cahn [2.518] were the first to study a puzzling new alloy of Al and Mn, prepared by rapid solidification from the melt, which had a fivefold symmetry axis. Subsequently, quasicrystalline modifications of several alloys have been discovered (see Section 3.1.1.). It has

been suggested that the formation of the quasicrystalline state can be explained by multitwinning or disorder phenomena [1.48]. Certainly, they are noncrystalline in the ordinary crystallographic sense, but they do not satisfy the criteria for an amorphous state, because long-range periodicity is still present. Therefore, these materials have been excluded from the scope of this book.

Anti-glasses are closely related to the CaF_2 -type structure, e.g., metastable $\text{SrTe}_5\text{O}_{11}$, prepared by quenching from the melt. They are characterized by random variation of the short-range order [1.49], [2.519]. In the structure of $\text{SrTe}_5\text{O}_{11}$ the Te and Sr atoms are randomly distributed over the Ca positions, and O atoms and Vacancies over the F positions of the CaF_2 structure [2.519]. This high degree of short-range disorder contrasts with the pronounced long-range order.

2.1 Methods of Preparing Amorphous Solids and Glasses

An amorphous or vitreous substance, even with identical chemical composition, differs from the crystalline state by its higher energy content. The short-range order regions of a crystalline solid often continue to exist even after melting. On the other hand, frequently the transition to the liquid state is accompanied by reconstructive structural changes in the first coordination sphere. Smaller units usually result from degradation, primarily in the gas phase, in the course of dissolution, and particularly at high temperatures.

Consequently, amorphous or vitreous solids can be obtained from the liquid state, i.e., from a melt or solution, or from the gas phase, provided that the formation of a periodic arrangement of units through the process of

nucleation and crystallization is prevented. The higher free energy of the melt, solution or gaseous state is stored, at least partly, in the solid state. This process is sometimes called freezing in this context. On the other hand, by supplying energy to crystalline solids they can be converted to the amorphous or vitreous state without passing through the liquid or gaseous phases. A survey of unconventional methods for preparing noncrystalline solids has been given by Secrist and Mackenzie [2.2]. The different variants are clearly shown in Figure 2.1 according to a proposal by Roy [2.3] and Owen.

Glasses are obtainable by sufficiently rapid cooling or quenching of melts (1) or by drying of gels from solutions (2). Processes of precipitation from solutions often lead to amorphous precipitates (3), as in the cases of red amorphous selenium, sulphides of As, Sb, Ge, Sn, and numerous other metals, or many metal hydroxides. Electrolytic separation using a high current density (4) leads to amorphous layers, such as amorphous germanium. The first examples of metallic glasses were obtained by this means. The preparation of so-called explosive antimony is an example of this kind. With regard to methods starting from the gaseous phase, the most important of these are the several variants of thermal evaporation and condensation in high vacuum (5), cathode sputtering (6), and deposition of amorphous layers in glow discharge processes (7). Reactive vapour deposition (8), too, has assumed some importance in specific cases, for example in the formation of vitreous silica or amorphous SiO_2 layers through hydrolysis of SiCl_4 or through pyrolysis of SiCl_4/O_2 mixtures. Vitreous silica films or SiO_2 layers can also be generated by the direct oxidation of silicon monocrystals at the surface (9). Crystalline solids are also converted to the amorphous state by the influence of shock waves (10) or intense irradiation (11) with neutrons or ions. Amorphous states are often formed during solid-state decomposi-

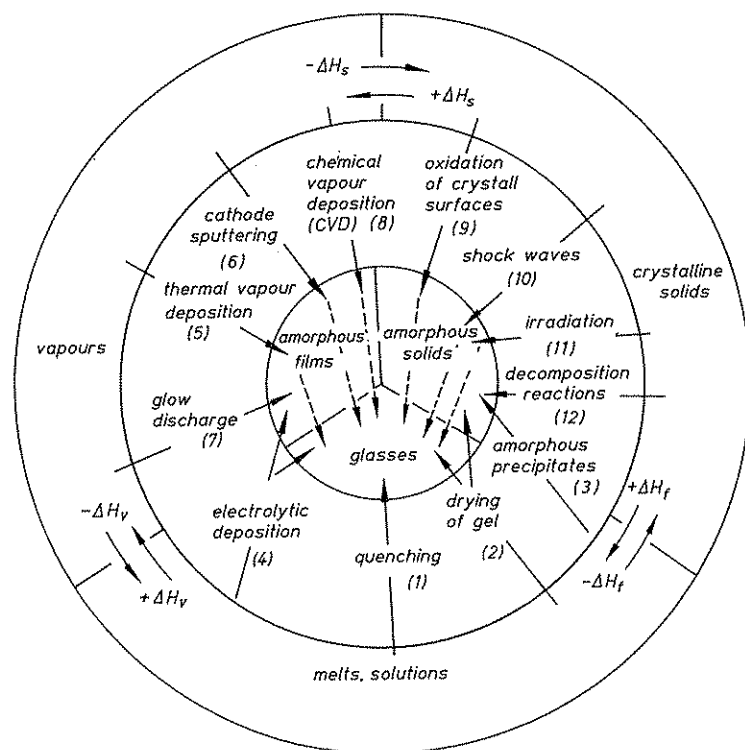


Fig. 2.1. Paths of formation of vitreous and amorphous solids from melts or solutions, vapours, and crystalline states of substances, according to Owen. More details are given in the text.

tion reactions (12), such as the dehydration of kaolinite. Finally, the mechanical treatment of crystalline solids, such as grinding and polishing, also leads to strongly disordered and amorphous surface layers. An awareness of these reactions is essential for some important technological processes.

The scope of this book is mainly restricted to those vitreous or amorphous solids that are obtained in their compact state or as coherent thin films up to several micrometres in thickness, of uniform composition, and of at least nearly homogeneous and isotropic structure, such that easily comprehensible structure-property correlations can be established. The arrows in the inner circle of Figure 2.1 indicate that, by a suitable choice of preparation con-

ditions or by subsequent annealing, the amorphous films and layers can be converted to a modification very close that of compact glasses, such as are obtainable from a melt.

2.1.1 Glasses from the Melt

The problem in preparing a glass from the melt is to maintain the homogeneous and isotropic state of the melt even during cooling, which means that nucleation and crystal growth must be suppressed. In industrial processes, the cooling of a glass melt is often combined with moulding. The rates of nucleation and crystal growth pass through a maximum at different temperatures below the

liquidus temperature (cf. Section 2.3.1.1 and Fig. 2.25)

Consequently, the cooling rate must be sufficiently high to suppress such events in the particularly critical region where the two curves overlap. Nevertheless, this condition also applies outside that region because of the random character of the nucleation and crystallization processes.

Turnbull [2.4] stipulates the complete absence of crystal nuclei in the given volume as the condition for vitrification. The critical cooling rate in such cases depends on the volume of the melt. Other authors [2.5] still define melting products as glass even if they contain up to one crystal nucleus per cubic centimetre. Uhlmann [2.6] proposed a crystalline volume fraction of 10^{-6} as the critical limit. The formation of glass from the melt thus requires conditions by which the kinetics of nucleation and crystal growth processes can be made inefficient. Experience shows that the trend to vitreous solidification of melts is a function of viscosity in the range of the liquidus temperature and of steepness of viscosity increase in response to falling temperature. The melt, supercooled and still plastically deformable, is converted to a solid with shape elasticity, i.e., the vitreous state, in the region of the transition temperature. Even the supercooled melt is thermodynamically metastable relative to the crystalline state. However, in glass the supercooled melt is present in its frozen state.

2.1.1.1 Oxide Glasses

A wide variety of industrial glasses for packaging, household uses, building and construction, electrical engineering, and optical applications, are manufactured in large industrial plants by the processing of melts, mainly in the open air. The technological methods are highly developed; they are described in detail in monographs and manuals on glass technology [2.7 to 2.9].

Scientific investigations cover a wide range of furnace systems with direct or indirect heating. The choice of suitable crucible materials is often problematic, especially in cases where the chemical resistivity of noble metals, such as platinum, cannot be guaranteed because of possible interaction with the melt. Other difficulties often result from the volatility of certain components and resultant concentration gradients in the melt products. Careful adjustment of an equilibrium in the melt, for example by stripping of volatile components out of certain batch ingredients (clarification process), has proved to be important for reproducible production of homogeneous glasses, as also have precautions against possible contamination by partial decomposition of the crucible wall or from impurities present in the working environment.

The most important glass-forming oxides and BeF_2 are listed in Table 2.1, together with some data on their melting and glass transition behaviour.

Table 2.1. Glass-forming oxides and BeF_2

	Melting temperature T_S (K)	Glass transition temperature T_G (K)	Heat of fusion ΔH_S (kJ mol^{-1})	Viscosity η at T_S (dPa s)
SiO_2	1995	1495	8	10^7
GeO_2	1389	853	17.2	7×10^5
B_2O_3	723	550	23	10^5
P_2O_5	853	537	71	5×10^6
As_2O_3	585	420	18.7	10^6
BeF_2	823	523	41.2	$> 10^6$

The combination of these glasses and BeF_2 and the addition of one or more metal oxide components leads to the great variety of industrial utility glasses. The number of possible combinations is extremely large, and developments in this direction are far from exhausted, since not only can alkaline and alkaline earth oxides be included in the melts, but also transition metal oxides and oxides of main group elements, such as Al_2O_3 , Ga_2O_3 , Sb_2O_3 , Tl_2O , PbO , Bi_2O_3 , TeO_2 , and even sulphates and chlorides, as well as numerous fluorides.

This wide area needs to be treated in a separate chapter. Relevant publications [1.1 to 1.5] have been mentioned in the Introduction.

One particular group of oxide glasses, first mentioned in papers by Rawson, Stanworth et al. in 1954 [1.25, 2.11], exhibits electronic conductivity. These glasses contain transition metal cations at medium levels of oxidation, e.g. not only Ti^{IV} but also Ti^{III} , and not only V^{V} but also V^{IV} , in large or even predominant amounts. Such melts are extremely sensitive to oxidation. Their preparation requires the careful avoidance of moisture, airborne oxygen, CO_2 , and other oxidizing or reducing substances.

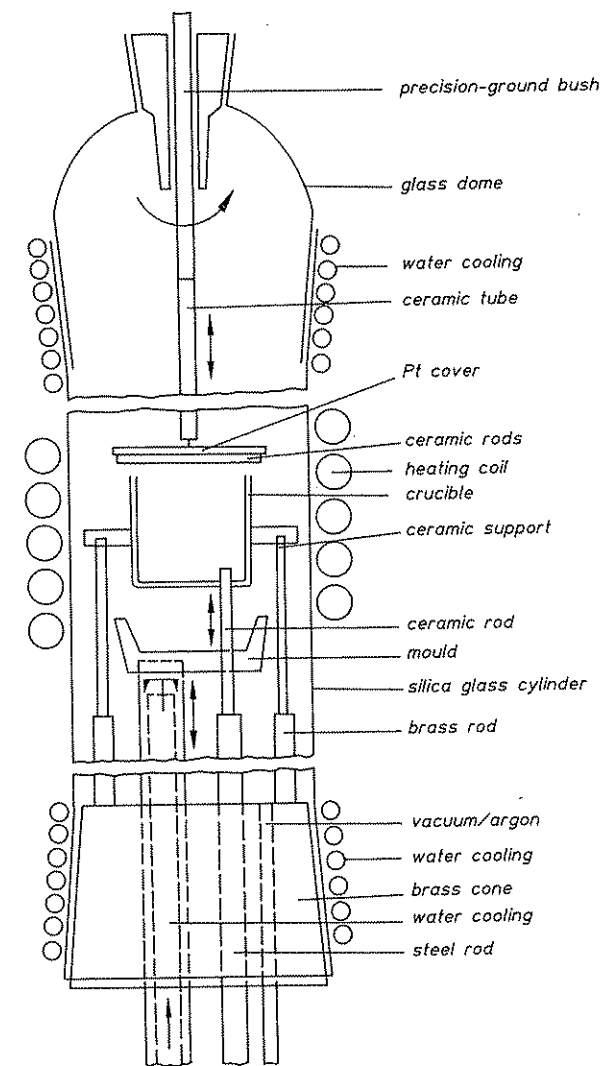
Figure 2.2 shows the essential parts of a quartz tube for this purpose (diameter 70 mm, length 600 mm), with inserts with movable lead-throughs fitted to the upper and lower sockets. The apparatus is vacuum-sealed, so that a clean argon atmosphere can be generated. The ground connectors are water-cooled to avoid thermal decomposition of sealing grease. The upper lead-through allows the melt to be stirred through an opening in the crucible lid, so that the latter can be lifted before casting. The crucible (90% Pt, 10% Rh), with inductive heating and capacity of 50 ml, is supported on two laterally welded cylindrical supports, allowing it to rotate. A rod can be inserted from below to tilt it to an inclined position, so that the slid-in water-

cooled mould can be emptied. Oxidation-sensitive glass melts, with their mean oxidation number prespecified in the mixture for the transition metal cation, can thus be melted and cast with good repeatability [2.12].

2.1.1.2 Chalcogenide Glasses

An extremely wide range of entirely new non-oxidic glasses based on vitreous selenium has been described over the past thirty-five years. Earlier important developments were the discoveries of arsenosulphide glass as an infrared-transmitting medium by Frerichs [2.13] about 1950, and of the semiconducting glass TlAsSe_2 during studies of the $\text{Tl}_2\text{Se} \cdot \text{Sb}_2\text{Se}_3 \cdot \text{Tl}_2\text{Se} \cdot \text{As}_2\text{Se}_3$ system by Goryunova and Kolomic [1.20, 2.14] in 1955. These glasses are sulphides, selenides, and tellurides of the elements of main groups IV and V, especially of Si, Ge, P, As, Sb, and combinations thereof, and combinations between these and the halogens, chalcogens or chalcogenides of heavy metals such as Hg, Ga, In, Tl, Sn, and Pb. The mechanical strength and thermal stability of such glasses are much lower than those of oxide glasses, and the thermal expansion, temperature coefficient of the refractive index, and relative photoelastic coefficient are much higher. Their transparency to infrared radiation, on the other hand, generally increases towards smaller wavenumbers owing to higher atomic masses and smaller bonding force constants [2.15, 2.16]. The decrease in mean bonding energy, associated with increase of atomic masses in homologous series of the Periodic System, leads to reduction of the band gap towards the oxides. Apart from a few exceptions, such as yellow GeS_2 and red As_2S_3 glasses, chalcogenide glasses absorb in the entire visible spectral region and are, consequently, opaque black. Thermal activation of charge carriers leads to an electrical conductivity which can sometimes be remarkably high. Glasses with conductivities of, for example, $10^{-3} \Omega^{-1} \text{cm}^{-1}$ at 298 K. have been

Fig. 2.2. Apparatus for melting oxidation-sensitive oxide glasses according to [2.12].



discovered. Chalcogenide glasses, in addition to electronically conducting oxide glasses, are thus a second group of vitreous substances with semiconductor properties. Their high reflectivity leads to some of them having a highly glossy appearance.

Suitable crucible materials for the preparation of chalcogenide glasses are graphite or vitreous carbon, as well as oxides with high

melting points, such as vitreous silica ampoules. The comparatively high melting energy, together with the relatively low melting temperatures of the chalcogenides, means that crucible wall corrosion of the SiO_2 ampoules is much lower than in the case of oxide melts. Operation in closed systems under anaerobic conditions is again essential because of the considerable vapour pressure of chalcogenide

melts and the tendency to react with oxygen, particularly at higher temperatures. Consequently, chalcogenide glasses are produced by melting the corresponding element mixtures in silica glass ampoules under vacuum. These ampoules are rotated in the furnace for better homogenization. In the case of a fixed ampoule, the furnace is periodically tilted. For melt quenching, the ampoules are thrown into a cooling liquid or cooled outside the furnace in the open air, or according to any other temperature-time programme. The relatively high coefficient of thermal expansion induces internal stress in the samples, so that before mechanical treatment they must be carefully annealed close to the glass transition temperature and then slowly cooled down to room temperature.

Important glass-forming chalcogenides are listed in Table 2.2. Vitreous selenium and some other glass-forming compounds, which belong to the pnictides, are also included. It can be seen that only As_2S_3 and, to some extent, As_2Se_3 , have viscosities close to the melting point which can be compared with those of the oxides (see Table 2.1). The other compounds are characterized by a considerably increased tendency towards crystallization in the region of supercooling.

2.1.1.3 Metallic Glasses

Vitreous metal alloys obtained from quenching of melts were first described in 1960 by Klement, Willens, and Duwez [1.27]. Thin vitreous films of Au_3Si could be produced by means of unusually high cooling rates. A great variety of vitreous alloys of transition metals T, predominantly with non-metals or semi-metals M, have become available since then. Their composition often lies between T_5M and T_3M . Other groups of metallic glasses are also known (see Section 3.1.1.1).

Several technological systems have been developed to give cooling rates up to $10^{10} K s^{-1}$. The number of inorganic substances that could be converted to the amorphous or vitreous state was greatly increased as a result of this development. In particular the investigation of metallic glasses, of particular interest for certain applications, was greatly stimulated by the introduction of these procedures. Reviews can be found in papers by Güntherodt [2.17] and by Handrich and Kobe [2.18].

The splat-quenching or gun technique is based on the propagation of a shock wave spreading in the vacuum space of the apparatus after the sudden rupture of a foil (see schematic drawing in Figure 2.3 a). This hits

Table 2.2. Selenium, glass-forming chalcogenides, and some pnictides.

	Melting temperature T_S (K)	Transition temperature T_G (K)	Heat of fusion ΔH_S ($kJ mol^{-1}$)	Viscosity η at T_S (dPa s)
Se	493	305	6.23 ± 0.17	22.1
P_4Se_4	603	455	—	—
As_2S_3	592	447	28.7 ± 1.3	$10^{5.1}$
As_2Se_3	648	445	40.8 ± 1.3	—
As_2Te_3	685	380	55.8 ± 1.5	—
GeS_2	1123	765	—	—
$GeSe_2$	1013	665	—	40
$CdAs_2$	894	545	—	—
$CdSiAs_2$	—	760	—	—
$CdGeP_2$	1073	715	—	—
$CdGeAs_2$	943	655	—	—

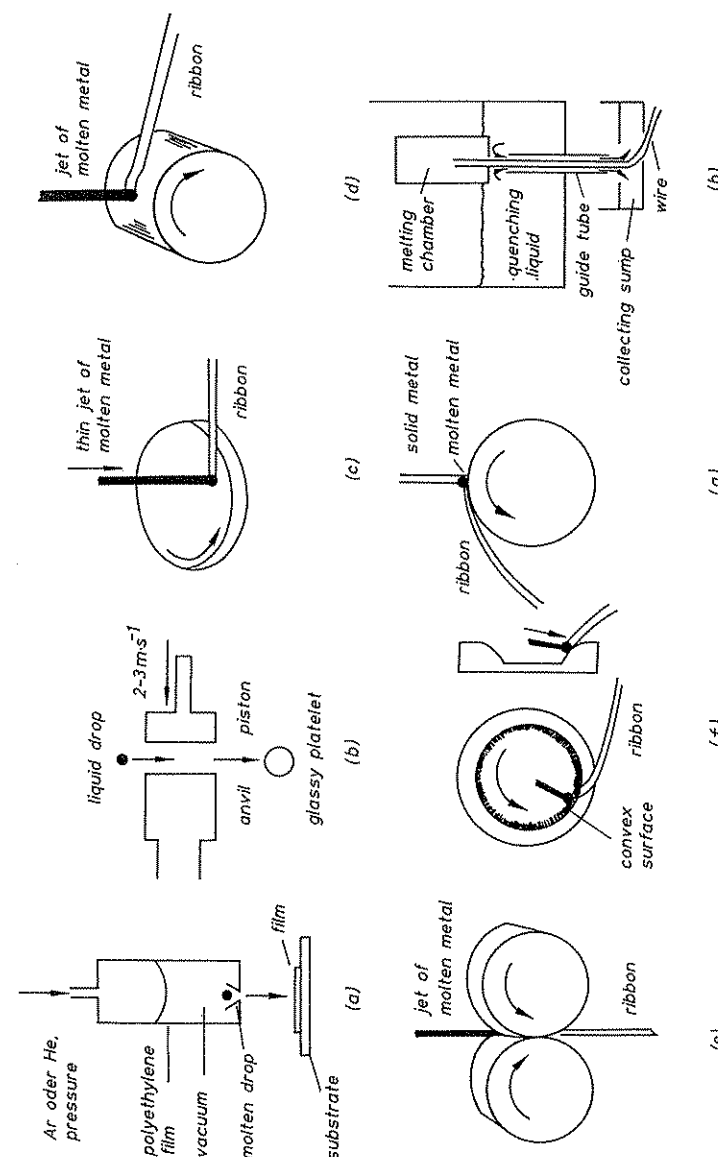


Fig. 2.3. Process variants for producing metallic glasses.

the melt and drives it through a small opening onto a cooled substrate, such as a copper plate.

This method was first used by Duwez and co-workers [2.19], and different variants have been described more recently elsewhere [2.17].

In the piston-and-anvil method, melt drops are allowed to fall, either freely or accelerated by the gun technique, between a stationary anvil and a movable piston. The piston strikes the anvil with a velocity of $2\text{--}3\text{ m s}^{-1}$, compressing the drop into a thin platelet, as may be seen from Fig. 2.3 b [2.20].

Melt spinning processes have the advantage of allowing the continuous production of thin tape-like foils [2.21]. The molten alloy passes through a nozzle under the effect of external gas pressure and impinges on a cooled, rapidly moving substrate, such as a rotating disc (Fig. 2.3 c) or a rotating cylinder (Fig. 2.3 d), or else it is rolled (roller-quenching) between two rapidly rotating rollers, as in Fig. 2.3 e [2.22]. In the case of centrifugal spinning, the liquid jet strikes the concave inner surface of a rapidly rotating drum, as shown in Fig. 2.3 f

[2.23]. The centrifugal forces ensure good thermal contact, the curved surface at the same time ensuring rapid lifting up of the tape from the substrate. In other arrangements that have been described [2.18], solids of rod shape are melted at the point of contact with a rotating disc or roller (melt extraction), so that no melting crucible or outlet nozzle is required (see Fig. 2.3 g [2.18]).

Wires and similar forms can be produced by the free jet spinning method, in which a thin jet of the melt passes directly through a cooling liquid and enters guide tube which is also cooled, as shown in Fig. 2.3 h [2.21]. Wires and tapes of metallic glasses can be manufactured by such methods in continuous processes, with a typical output capacity of 2 km per minute.

2.1.1.4 Variation of Cooling Rate of Glass Melts

A summary of cooling rates used in the production of inorganic glasses from melts is given in Table 2.3. Industrial and optical glasses are subjected to very precise annealing in accordance with the specific demands on homogeneity and absence of stress. This is possible by means of specially designed cooling furnaces controlled with a particular programme. Cooling must be sufficiently slow, even above the transition temperature, so that convection and hydrodynamic instabilities in the melt can be avoided. Otherwise, parts close to the surface of the melt, which always have a slightly altered composition, would enter the volume in an unchecked manner and cause optical inhomogeneities, such as striations, rendering the glass casting unsuitable for optical purposes. It must be ensured that all parts of the glass body are subjected to a more-or-less homogeneous temperature treatment. This requires temperature gradients from the centre to the surface to be minimized, which in turn demands the smallest possible cooling rates, even below the transition tem-

Table 2.3. Typical cooling rates of glass melts.

Cooling rate q (K s ⁻¹)	Method
10^{-5}	Annealing of large telescope mirrors
approx. 2×10^{-4}	Annealing of optical glasses
$10^{-3}\text{--}10^{-2}$	Annealing of ordinary glasses
1–2	Air exposure of chalcogenide melts of 10–20 g in quartz ampoules (wall thickness 2 mm)
8–10	In water at 273 K
35	1 g (ampoule wall thickness 0.5 mm) in water
approx. 180	0.015 g in thin-wall ampoule in water [2.23]
approx. 10^3	Spray-cooling of melts
$10^5\text{--}10^6$	Melt-spinning methods
$10^6\text{--}10^7$	Piston-and-anvil technique
$10^6\text{--}10^{10}$	Splat-cooling methods

perature. Consequently, melts for industrial and optical glasses must meet very high demands on their resistance to recrystallization.

Higher rates of cooling are used when investigating trends in glass forming behaviour of particular systems of substances. The melt batches are often smaller, so that strains do not cause problems in the early phases. Also, in these cases, the melt is cooled down as far as possible before casting or quenching. With sufficiently high viscosities and suitable container dimensions, the formation of convection flows in the melt can be suppressed to a large extent. Strain can be largely eliminated by subsequent annealing. The sometimes present considerable vapour pressures for chalcogenide melts in molten silica glass ampoules require the greatest of care. Quenching from too high a temperature results in a pressure drop above the melt, and thus often in boiling, so that the resultant product is foamy or interspersed with bubbles.

If a melt of some dozens of grams is left to cool in air, for example by casting it in a non-preheated mould, or simply by taking the ampoule with the chalcogenide melt out of the furnace, it must always be remembered that

the outermost zone of the substance is subject to faster cooling than the inner part, so that the sample no longer has a homogeneous thermal history. Only an integral mean value of the cooling rate can then be specified; it depends on the heat capacity and heat conductivity of the system, and thus on the mass and mean molar mass of the melting batch, and on the dimensions of the mould in which the melt is cast, or, in the case of chalcogenide melts, on the shape and wall thickness of the vitreous silica vessels.

An arrangement for determining the cooling rate of chalcogenide melts in cylindrical vitreous silica ampoules is shown in Figure 2.4, together with the cooling curves obtained for melts of 10–20 g in ampoules with a wall thickness of about 2 mm quenched in air (curve a), and in an ice-water mixture (curves b), in the latter case for three different melt temperatures.

It is advisable to record the cooling rate for comparison, because the freezing process depends on the rate at which the sample passes through the supercooling range, i.e., the temperature region between the melting temperature T_m and glass transition temperature T_G .

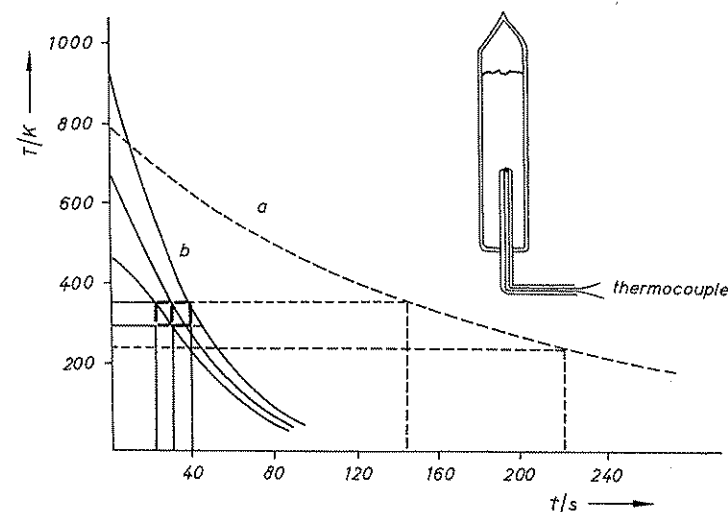


Fig. 2.4. Arrangement for determining the cooling rate of chalcogenide melts.

The range chosen for Fig. 2.4 is $T = T_G \pm 50$ K. In the region of about 300 K, the resulting rates were 2 K s^{-1} for cooling in air (curve a) and to $8\text{--}10 \text{ K s}^{-1}$ for quenching in water (curves b). Melts of 1 g in small ampoules with thin walls (about 0.5 mm) gave a cooling rate of 35 K s^{-1} . Similar values are reported by Cornet and Rossier [2.24]. Cooling rates can be doubled or trebled by quenching in cooled concentrated sodium hydroxide solution.

A further increase in cooling rate is possible by reduction of the melting batch mass, or by improving the heat dissipation by melting without vessels. The melt can then be brought into direct contact with a cooling liquid or a cooled substrate.

Melting by the spray-cooling method is carried out in a quartz tube with an opening of about $100 \mu\text{m}$ in the base [2.25]. The melt is sprayed by externally applied pressure into vigorously stirred oil bath. This gives vitreous droplets with diameters of 100 to $300 \mu\text{m}$.

The highest cooling rates can be achieved by means of the methods described in Section 2.1.1.3. Davies and Hull [2.26] have ported that rates as high as 10^{10} K s^{-1} are possible by quenching metal melt layers with thicknesses of about $0.15 \mu\text{m}$. Such data are based on the observation of hydrodynamic structures forming in the melt due to extreme non-equilibrium conditions during quenching [2.18]. Sargeant and Roy [2.27] used the same method and succeeded in converting V_2O_5 , TeO_2 , WO_3 , and MoO_3 to the vitreous state. Nassau [2.444] recently reported on the quenching of melts of vitreous modifications of LiNbO_3 , KTaO_3 , $\text{Y}_3\text{Fe}_5\text{O}_{12}$, $\text{Li}_4\text{CdK}(\text{SO}_4)_4$ and numerous other oxide phases at rates of about 10^7 K s^{-1} .

Roller quenching of $\text{BaO-B}_2\text{O}_3\text{-Fe}_2\text{O}_3$ glasses has become a technologically important process. Annealing of the glass flakes obtained gives mono-sized $\text{BaFe}_{12}\text{O}_{19}$ crystalline powders which have found application as magnetic pigments for tapes [2.473, 474]. Preparation of $\text{YBa}_2\text{Cu}_3\text{O}_{7-\delta}$ superconduc-

tors using methods of glass technology has been also proposed [2.475].

2.1.2 Amorphous Solids from Solutions

Dissolved substances can be converted to solids by evaporation of the solvent, by temperature variation, by addition of precipitants such as liquids that reduce the solubility by modifying the polarity or donor strength, or by other precipitating reagents. Cathodic or anodic separation is also an important method.

Amorphous substances are formed from solutions when the conditions change at a sufficiently high rate, followed by strong oversaturation, that there is often not enough time for the generation of crystalline nuclei and their growth. Such substances often pass through colloid-disperse states. Particle enlargement by coagulation is inhibited, which is often the cause of the well known difficulties in filtration of precipitation products. The solution, in certain cases, solidifies as a gel, which can then be converted continuously to an amorphous solid. Substances separated from solutions in noncrystalline form show an extremely wide variety of behaviour. In contrast to those situations in which amorphous states cannot be obtained except by rapid addition of the precipitant, or by electrolysis with high current density, there are many other chemical substances which preferentially come out of solution in noncrystalline form (cf. Section 3.2.4.2).

2.1.2.1 Glasses Formed by Homogeneous Precipitation of Gels

The advantages of coprecipitation of substances such as different oxides, hydroxides, or oxide hydrates, for subsequent chemical conversion to a solid, have long been known. The components are in very close contact in the precipitation product. Even a molecular-dis-

perse distribution can be found as a result of compound of mixed phases, so that the diffusion paths for solid reactions are relatively short. Conversion requires shorter times or significantly reduced temperatures.

Roy [2.28] suggested the utilization of these possibilities for glassmaking. Dislich [2.29] reported in detail, showing that, or instance, solutions of $\text{Si}(\text{OC}_2\text{H}_5)_4$, $\text{Al}(\text{OC}_4\text{H}_9)_3$, NaOCH_3 , and KOC_2H_5 in ethanol can be converted to a gel by hydrolysis, until the step-by-step degradation of this gel results in glass. Temperatures up to the glass transition temperature of about 800 K were found to be sufficient. The properties are largely the same as those of products obtained from a melt. Borosilicate and aluminoborosilicate glasses have also been obtained by the same method [2.427]. The products are then shaped by pressing at temperature T_G without passing through the temperature region for maximum crystallization rate or for the initiation of phase separation phenomena (see Section 2.3.1). This method makes it possible to prepare glasses not obtainable from the melt phase, such as $\text{TiO}_2/\text{SiO}_2$ or $\text{ZrO}_2/\text{SiO}_2$ glasses with comparable component fractions [2.428, 2.429]. Practical applications to the production of large-area, reflection-reducing coatings have been developed [2.430]. Zarzycki [2.455] is involved in theoretical approaches to describing the conversion of gels to the vitreous state.

Several conferences summarizing advances in the last few years have taken place (see, e.g., [1.40]). A fundamental review has been given by Hench and West [2.476]. The structure of sol-gel-derived glasses is discussed in a review paper by Brinker [2.514]. Schmidt [1.41] has developed a new class of inorganic-organic vitreous materials using sol-gel preparation techniques. The so-called Ormoceres, formed by cocondensation and copolymerization of silicones and organic monomeric or oligomeric compounds, have properties that can be tailored over a wide range to suit specific applications.

2.1.2.2 Amorphous Precipitates

The generation of amorphous precipitates is a widespread phenomenon in the chemistry of aqueous solutions. It is usually regarded as a nuisance, so that attention has been focused on identifying conditions that give stoichiometric, easily filterable crystalline precipitates. Silicic acid, various metal hydroxides or oxide hydrates, and many basic salts, all of them amorphous, result from separation without a well-defined chemical composition. Because of the large surface, other ions in the solution are easily precipitated by adsorption or chemisorption, which often leads to problems in separation for analytical purposes.

On the other hand, there are compounds with stoichiometric composition which always occur in amorphous form after precipitation from aqueous solutions, such as the sulphides As_2S_3 , As_2S_5 , Sb_2S_3 , Sb_2S_5 or GeS_2 . These can even be used for the gravimetric determination of As, Sb or Ge owing to their sparing solubility and stoichiometry. As_2S_5 and Sb_2S_5 are so far only known as amorphous compounds; the same also applies to MoS_3 , MoSe_3 , WS_3 , WSe_3 , and V_2S_5 . Ge_2S_3 and Ge_2Se_3 are obtained as amorphous precipitates from solutions of thiohypodigermanate and selenohypodigermanate, but can also be obtained as vitreous compounds from the melt (see Sections 3.2.2.4, 3.2.2.5, and 3.2.4).

Amorphous precipitates of defined composition M_2SnTe_4 ($\text{M} = \text{Cr, Mn, Fe, Co}$) have recently been reported. They can be obtained from the combination of anhydrous M^{2+} and SnTe_4^{4-} solutions, and they show metallic conductivity after compaction by pressing [2.456].

2.1.2.3 Electrolytic Deposition of Amorphous Layers

The passivation of metal surfaces by anodic oxidation is associated with the formation of closely adhering and largely amorphous oxide

layers which protect the metal from further oxidative attack. The thickness is of the order of 0.1 μm . The passivation of aluminium is of great practical importance. Transparent amorphous Ta_2O_5 films are stable up to 923 K, before crystallization begins [2.30].

Amorphous metal alloys of phosphorus with nickel or cobalt were first obtained as cathode deposits during electrolysis with high current density [2.31].

An excellent paper on enthalpy studies and structural evolution of electrolytically produced amorphous $\text{Co}_{1-x}\text{P}_x$ alloys has been published by Flechon et al. [2.477]

Tauc [2.32] reports on the separation of amorphous germanium layers by cathodic reduction during electrolysis of GeCl_4 in glycol. These layers are, however, heavily contaminated with impurities from the solution. The so-called "explosive antimony" generated during electrolysis of acidic SbCl_3 solutions still contains considerable amounts of bonded chlorine, and thus is really an antimony subchloride. Heating causes explosive dismutation accompanied by evaporation of SbCl_3 . Electrochemical methods are hardly suitable for the preparation of clean amorphous layers.

2.1.3 Amorphous Layers from the Gaseous Phase

The most important methods for depositing amorphous or vitreous layers by the condensation of vapours on suitable substrates are thermal evaporation, cathode sputtering, decomposition reactions occurring in glow discharges, and reactions between different gaseous components, whose products are then as solids. There is a wide diversity of possible preparation conditions, so that even single-component systems permit a great variety of amorphous structures to be produced. This variation is often affected in non-reproducible ways by contamination through impurities or

by the incorporation of foreign substances. Consequently, ensuring the purity of such layers and monitoring their composition by analysis is particularly important. Many publications have neglected this aspect.

Multicomponent systems require careful verification of the vertical and horizontal homogeneity. Little is known about the mechanisms of formation. Investigations of the kinetics of evaporation and the mechanism of condensation are available [2.33 to 2.35] for only a few simple systems, such as some elements or certain defined compounds. Even in those cases, the mass-spectrometric analysis of vapour composition indicated a broad spectrum of different species, so that the results thus obtained can only be regarded as an integrated average.

Systems whose melts show a tendency towards vitreous solidification usually still tend to form non-periodic structures, even when solidified by separation from the gaseous phase. In such cases the materials formed have a nearly constant chemical composition. Substrate cooling is conducive to the process, because the suppression of the formation of crystal nuclei with the ability to grow is similarly important in these methods of preparing amorphous or vitreous substances. The stronger the crystallization tendency in a given system of substances, the lower the temperature required to give an amorphous deposit. For condensation on substrates cooled with liquid helium the higher entropy of the vapour and the extreme quenching conditions lead to the formation of vitreous or amorphous modifications, even with systems for which all other methods had previously failed. Some examples are Mg, Zr, Hf, Nb, Ta, Mo, W, Re, and Cd.

2.1.3.1 Methods Using Thermal Evaporation Under Vacuum

Evaporation is a stochastic process which can be described in the context of the kinetic

theory of gases. The state of equilibrium is characterized by elastic collisions of particles at the interface between the condensed and the gaseous phases (exchange of heat) and by the release and separation of particles on the surface (exchange of work).

Evaporation under Equilibrium Conditions (Knudsen Conditions). The equilibrium is essentially maintained under the conditions of evaporation from a Knudsen cell, as the opening in the evaporator is small relative to the surface area of the source. The mass flow rate R_m for an ideal gas in one direction can be expressed by the gas-kinetic equation:

$$R_m = \frac{1}{4} \frac{m}{v} \bar{u} = \left(\frac{M}{2\pi RT} \right)^{1/2} p \quad (2.1)$$

with M = molar mass, \bar{u} = mean velocity according to the Maxwell-Boltzmann distribution, $\bar{u} = (8 RT/\pi M)^{1/2}$, and $(m/v) = Mp/RT$. By measuring the mass loss as a function of time, the saturation vapour pressure can be determined. In the case of composite systems, Eqn. (2.1) is applicable to the partial mass flow rates R_{mi} and the corresponding partial pressures P_i , so that the vapour composition will usually vary with time.

Evaporation in Free Vacuum (Langmuir Conditions). Sources with larger openings, such as open crucibles or combustion boats, heated directly or indirectly, are used for evaporating larger quantities within a given time. Equilibrium conditions are no longer applicable. The evaporation process is determined by the rate at which the solid or liquid substance is degraded at the surface. This means that the kinetics of these processes, or even the transport of thermal energy to the place of reaction, determine the rate of the overall process. Eqn. (2.1) is used nevertheless, but modified by a factor $\alpha = R_m^*/R_m$ which, for obvious reasons, must always be smaller than 1.

$$R_m^* = \alpha \left(\frac{\bar{M}}{2\pi RT} \right)^{1/2} p \quad (2.2)$$

\bar{M} is the average molar mass of particles in the vapour jet. This means that fractionation effects are unavoidable in cases of incongruent evaporation and different vapour pressures of the decomposition products.

An activation parameter ΔE^* can often be calculated according to

$$R_m^* = A \exp(-\Delta E^*/RT) \quad (2.3)$$

from the temperature dependence of the rate of free evaporation in vacuum. It does not represent the evaporation enthalpy, but is an average describing the degradation reactions on the surface of the substance to be evaporated.

Effects of re-evaporation from the layer already deposited can largely be avoided if the substrate temperature is sufficiently low and the distance between evaporator and substrate sufficiently large. In other words, the experimentally determined evaporation rate R_m^* can be converted into a condensation rate R_k^* , taking into account the solid angle. The entire process can be represented consistently by an arrangement of this kind in cases where there is agreement with the condensation rate determined experimentally.

The lower the substrate temperature, the greater the risk of contamination by impurities that may originate, for example, from the environment of the evaporator system or from residual gases, especially from the working fluid of vacuum pumps. Furthermore, the deposited layers are relatively loose and sometimes even porous, so that their later contact with air leads to rapid changes. Condensation should be carried out at the highest possible substrate temperature and as slowly as possible, insofar as the glass transition temperature and the vapour pressure of the vitreous film allows this. Deposition rates of 0.1 to 0.5 nm s^{-1} at a substrate temperature of 298 K, e.g., in the evaporation of $\text{Ge}_4\text{Se}_5\text{Te}$, permit a sufficient surface mobility, so that relatively compact films can be produced. Their prop-

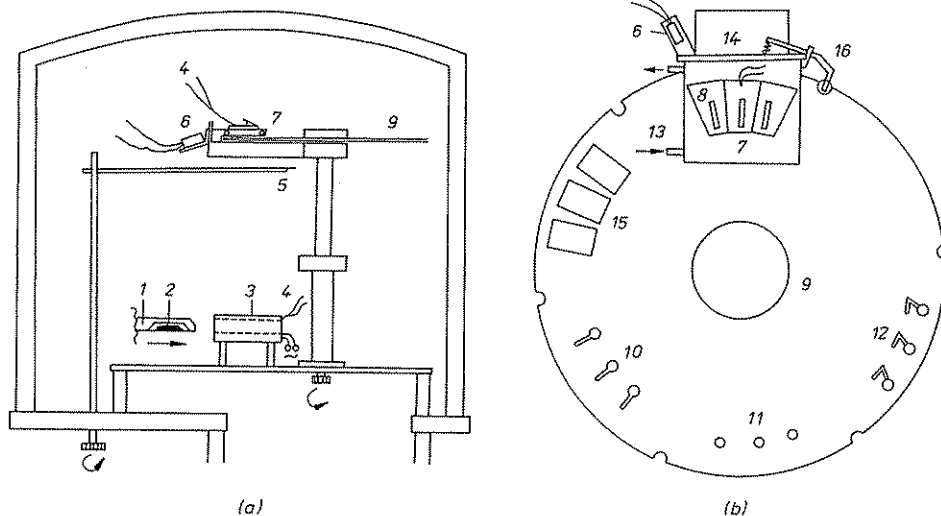


Fig. 2.5. Experimental arrangement for deposition of amorphous layers by thermal evaporation in vacuum according to [2.37]; (a) complete arrangement with rotatable substrate holder and masks; (b) details of mask.
(1) boat of Ta sheet; (2) substance; (3) preheated Cu block with opening

erties largely correspond to those of compact glass, so that an analogous structure can be assumed (see Sections 3.3.3.2, 4.1.3.6). For the preparation of amorphous Ge layers, similar rates of deposition at a substrate temperature of 470 K give best results.

Many different variants of evaporator arrangements have been described [2.36]. A possible arrangement for investigating the evaporation of vitreous Ge₂Se₃ and polycrystalline mixtures of GeSe and GeSe₂ is shown in Figure 2.5 a. The rotatable substrate plate (Fig. 2.5 b) has different masks and allows sample contacting in the same vacuum cycle. The layers required for the chemical analysis are obtained at the same time [2.37].

An initially surprising result is obtained on plotting the evaporation and condensation rates R^* against the reciprocal temperature, as shown in Figure 2.6 a. Although the homogeneous Ge₂Se₃ glass, introduced into the evap-

oration process with mean particle diameters between 0.3 and 0.7 mm, has a higher energy content than the crystalline GeSe/GeSe₂ mixture, the value for the activation energy of free evaporation of the supercooled melt (the T_G value is 608 K) is twice as high as that of the polycrystalline mixture [2.38]. The supercooled melt crystallizes at about 730 K. Under conditions of equilibrium evaporation, the latter would result in a lower evaporation enthalpy in the range of $T < 730$ K, and the sublimation enthalpy of the polycrystalline substance would be greater. However, in cases of non-equilibrium conditions of free evaporation, the kinetics of degradation and reorganization processes on the surface, or even the rate of supply of the necessary thermal energy, determine the temporal characteristics of evaporation. The differences are illustrated in Figure 2.6 b.

A largely intact network of Ge₂Se_{6/2} units

can be assumed to exist in glass or in the supercooled melt (see Section 3.2.2.5). On the other hand, the crystalline mixture has a heterogeneous structure with GeSe and GeSe₂ in a stratified lattice arrangement. Mass-spectrometric investigation has shown that the vapour consists mainly of GeSe and Se₂ molecules [2.38].

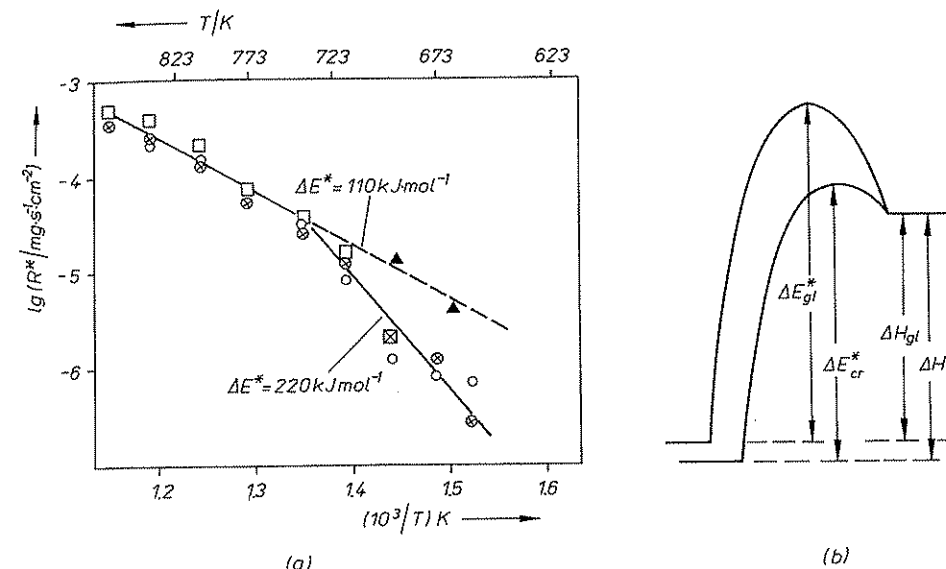
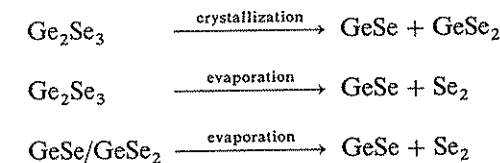


Fig. 2.6. a. Logarithmic plot of the evaporation rate R^* (O), condensation rate $R^\#$ (□), and deposition rate R^* (⊗), the latter measured after calibration with a quartz oscillator monitor, against the reciprocal temperature (according to Eqn. (2.3)) for evaporation

of a supercooled Ge₂Se₃ melt or an equimolar GeSe/GeSe₂ mixture (▲).
b. Comparison between enthalpies of evaporation ΔH_v and activation ΔE^* of crystalline and vitreous states: Although $\Delta H_{gl} < \Delta H_{cr}$, is $\Delta E_{gl}^* > \Delta E_{cr}^*$.

can be assumed to exist in glass or in the supercooled melt (see Section 3.2.2.5). On the other hand, the crystalline mixture has a heterogeneous structure with GeSe and GeSe₂ in a stratified lattice arrangement. Mass-spectrometric investigation has shown that the vapour consists mainly of GeSe and Se₂ molecules [2.38].



The evaporation rate R^* will depend on the slowest step of the complex reaction directly preceding the transition to the gaseous phase. The activation energy of free evaporation often considerably exceeds the evaporation or

sublimation energy, if the liquid or vitreous state of the respective substance has a macromolecular polymeric structure. This applies, for example, to amorphous arsenic, red vitreous phosphorus, or vitreous and monoclinic As₂O₃ [2.39]. Free evaporation of vitreous As₂O₃, for example, is characterized by a value of $\alpha = 2 \cdot 2 \times 10^{-6}$ [2.40]. Gutzov [2.41] emphasizes that the very low evaporation rate of glasses under Langmuir conditions with $10^{-5} < \alpha < 10^{-9}$ is a characteristic of the vitreous state.

Mass-spectrometric analyses of the vapour composition and careful analysis of deposited films as a function of the film thickness show that a composition that is time-independent can be achieved only by evaporation of the supercooled Ge₂Se₃ melt, i.e., below the crystallization temperature. Higher concentrations of GeSe are present in the vapour and in

the deposited layers, which means that some GeSe_2 will remain after decomposition of the $\text{Ge}_2\text{Se}_{6/2}$ units. The differences between GeSe and GeSe_2 in evaporation behaviour are, however, largely eliminated if vitreous Ge_2Se_3 is used. For evaporation of multicomponent systems in free vacuum, glasses with their relatively uniform surface, are preferred to polycrystalline mixtures of various substances. Homogeneous layers can be prepared, even in cases where deviations from the initial composition in the evaporator occur, if a sufficiently constant vapour composition can be maintained. This requires the evaporation to be stopped before altered concentrations in the residue begin to have a significant effect on the vapour jet composition. For example, fractionation effects can be reduced by using sufficient amounts of the substance introduced into the evaporator.

Electron or laser beam evaporation hardly offers any advantage in this respect. However, these methods are suitable for evaporation of small defined regions of a sample, or for attaining very high localized evaporation temperatures without introducing effects from the crucible wall or from the material of the evaporation source. However, the methods of flash evaporation can be used to largely eliminate fractionation effects.

Flash Evaporation and Plasma Jet Evaporation. In flash evaporation small particles of a substance are intensely heated, usually under free fall conditions, and evaporate very rapidly and completely. The result is a wide spectrum of fragmentation products, whose deposition on the substrate leads to amorphous layers with a high degree of disorder. Because of this sudden evaporation, small compact particles are carried along with the vapour stream and incorporated into the amorphous layer. The evaporator can be provided with internal baffles to avoid such effects, thereby ensuring that the deposited layers are made up of atomic or molecular components of the vapour. The vapour stream is thus subjected

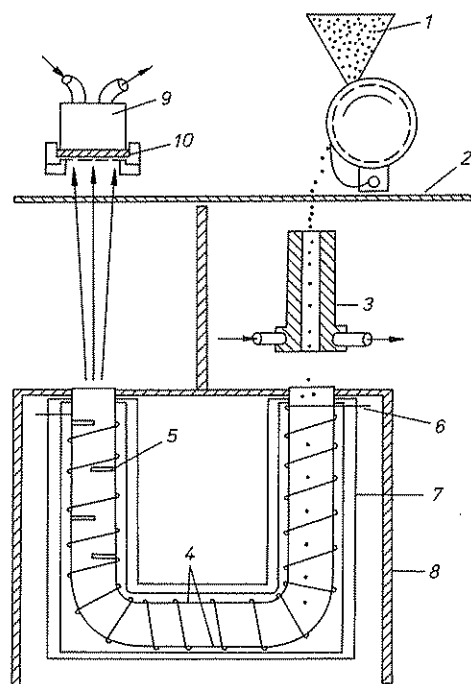


Fig. 2.7. Experimental arrangement for flash evaporation according to [2.42].

(1) granulated substance with metering unit; (2) heat shield; (3) cooled tube; (4) U-shaped vitreous silica tube with baffles (5); (6) filament heater; (7) heat shield; (8) cooled heat shield; (9) cooled substrate block with mask (10).

to frequent changes of direction, increasing its residence time in the zone of high temperature, so that complete evaporation becomes possible. Figure 2.7 shows an evaporator arrangement with an indirectly heated U-shaped quartz tube with offset baffles inside. This has worked well in the evaporation of chalcogenide glasses [2.42].

The method of plasma jet evaporation uses a high-temperature plasma for the evaporation of particles which are allowed to fall one at a time [2.43]. This leads to complete evaporation and also produces a vapour jet with a high velocity. Velocities up to 20 km s^{-1} in a narrow well-defined jet are possible by applying a strong electric field to induce emission

of ionized particles from the melt in high vacuum [2.44].

2.1.3.2 Amorphous Layers Generated by Cathode Sputtering

The production of amorphous layers by cathode sputtering uses an inert gas, usually argon, in which a gas discharge is generated at reduced pressure of 10^{-2} to 10^{-3} Pa [2.45–2.47].

The Ar^+ ions are accelerated in the field and hit the cathode at high speed. The cathode is coated with the substance to be volatilized. Atoms and smaller molecular fragments are detached from the surface of the target by thermal evaporation and also by direct collisions. The energy of the Ar^+ ions varies from several hundred to several thousand electron volts, depending on the applied field strength, and is thus much higher than the bonding energy of atoms within a solid structure [2.36]. Fractionation effects, frequently occurring in the thermal evaporation of multicomponent systems, are less likely if this method is used.

The evaporation results from the high ther-

mal excitation of the lattice, and is mainly localized in the immediate vicinity of impacting Ar^+ ions. The high energy density considerably reduces fractionation effects. However, vapour pressure differences cannot be ruled out completely even with this method. The impact mechanism is enhanced as the energy of the Ar^+ ions is increased, so that remaining fractionation phenomena decrease with the application of higher voltages.

More than 99% of the detached material consists of neutral particles. They are deposited as a thin film in the marginal zone of the gas discharge on a substrate positioned appropriately. Provided that cooling is adequate, amorphous layers of relatively consistent composition can be generated in this process, even from substances of complicated composition.

Typical arrangements with two and three electrodes are shown in Figure 2.8. In the former case (a) the plasma is generated between the electrodes by a DC voltage of 1–11.5 kV and at a gas pressure of 10–11 Pa. The layer is deposited on the anode, and is simultaneously exposed to the action of high-

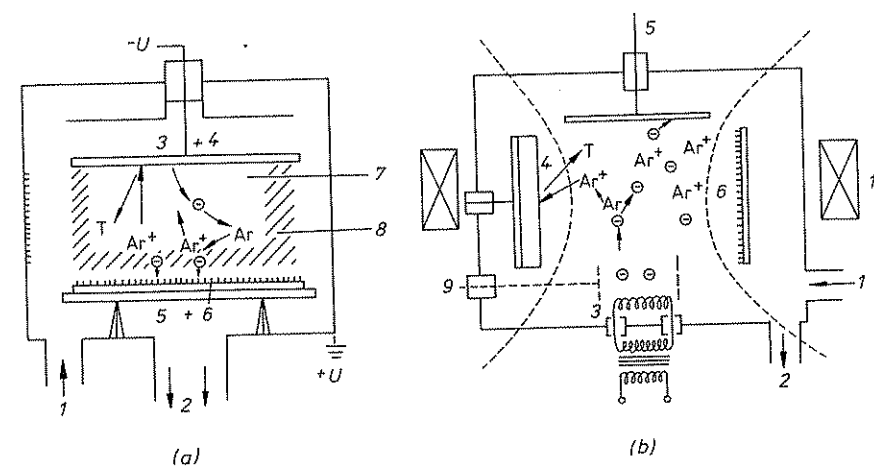


Fig. 2.8. Cathode sputtering, with diode arrangement (a) and triode arrangement (b).

(1) gas supply; (2) pump; (3) cathode; (4) target; (5) anode; (6) deposited layer; (7) cathode dark space; (8) positive column; (9) auxiliary anode; (10) magnetic coil and constriction of plasma.

energy electrons. In the triode arrangement (b), the electrons are captured separately by an anode. The Ar^+ ions are again extracted from the gas discharge zone in a DC voltage field of 1–2 kV (gas pressure 5×10^{-2} to 1 Pa). The contact between the plasma and the target or the substrate is reduced by an externally applied magnetic containment field.

The cathode sputtering of non-conducting or poorly conducting substances would lead to positive charging of the target, and the entire process would collapse within short time. Consequently, the sputtering of dielectrics requires a periodic supply of positive and negative charges, which can be accomplished, for example, by the application of an AC voltage. Frequencies around 10 MHz (radio-frequency sputtering) have proved to be suitable. This case is illustrated in Figure 2.8 b. Apart from the metallic glasses, amorphous films usually have low conductivities, and high-frequency cathode sputtering methods can be used in such cases.

The investigation of layers of chalcogenide glasses, such as the relatively complicated composition of $\text{As}_{0.30}\text{Si}_{0.12}\text{Ge}_{0.12}\text{Te}_{0.48}$, which can be produced by this method with

good reproducibility, has greatly stimulated research into electrical properties (see Section 4.1.3.7). Sputtering methods are well suited to the production of layers in multicomponent systems with considerable differences between vapour pressures of the components. However, considerable amounts of argon incorporated in the structure have been found in the amorphous Si and Ge layers made by cathode sputtering (see Section 3.1.2.3). The method cannot be regarded as useful if the layers have to meet very high demands on purity. The gas pressure required for maintaining the discharge, the resultant contamination, and also impurities from the environment, often considerably impair the purity of deposited layers.

2.1.3.3 Deposition of Amorphous Layers in a Glow Discharge

The preparation of amorphous layers by decomposition of certain gaseous substances or gas mixtures in a glow discharge is another plasmachemical process. Such methods have assumed industrial importance [2.48 to 2.50]. Plasmas are highly ionized gases, whose characteristic properties result from the differ-

ent mobility behaviour of ions and electrons. Electron temperatures in non-thermal plasmas can be up to four orders of magnitude above the temperature of the ions and neutral gas molecules.

A glow discharge is developed when an electric field of some hundred volts acts upon a gas in a sealed vessel or in a tube with internal flow at reduced pressure (about 10 Pa). The electron and ion densities are about 10^{10} cm^{-3} . The energy of the electrons, 1–10 eV, is 30 to 300 times greater than the mean thermal energy of the ions and neutral molecules. The high electron mobility leads to breaking of a great number of chemical bonds, so that chemical reactions are thus stimulated at relatively low temperature. Two experimental arrangements are shown in Figure 2.9, one with inductive and the other with capacitive supply of electrical energy. Ranges from 10 to 20 W in power and 1 to 100 MHz in frequency are typically used. The structure and properties of the deposited layers depend on various parameters, such as the substrate temperature, tube diameter, and the substrate position relative to the induction coil or the electrodes. The contact between the plasma and the deposited layer is of considerable importance.

This method has been used to deposit layers of metals such as tin or lead from $\text{Sn}(\text{C}_2\text{H}_5)_4$ or $\text{Pb}(\text{C}_2\text{H}_5)_4$ [2.51], and the deposition of tightly adhering amorphous layers of organic polymers has also been described in many publications [2.50]. Sterling and co-workers [2.52, 2.53] used the glow discharge method to deposit amorphous Si and Ge layers from SiH_4 and GeH_4 . The layers contain considerable amounts of Si–H or Ge–H bonds, and should thus really be understood as polycyclosilanes and polycyclogermanes with a high degree of cross-linking. The reproducible preparation of such layers demands very precise adjustment of the parameters mentioned above. The method has aroused particular interest by its ability to provide useful p–n

junctions in amorphous Si layers by the successive admixture of dopant gases such as PH_3 or B_2H_6 (see Sections 4.1.3.5 and 5.1.4).

Recently there has been growing interest in amorphous multilayers, so-called superlattices, that can be obtained by plasma chemical deposition from the gas phase [2.460, 2.461]. By periodically altering the composition of the gaseous phase, layers with thicknesses between 0.5 and 100 nm can be synthesized as a layer package in alternating sequences. There is a distinction between multilayer structures with periodic variation of composition, such as series of amorphous $\text{Si}(\text{H})/\text{SiN}_x(\text{H})$ layers, and those with periodic variation of doping, such as series of p–n junctions. They have unusual properties and can be expected to be used in the manufacture of components and in electrophotography (Chapter 5).

For example, by applying the glow discharge method to mixtures of SiH_4 and N_2O or of $\text{Si}(\text{OC}_2\text{H}_5)_4$ and O_2 , it is possible to produce thin coherent vitreous layers of SiO_2 . Use of $\text{B}(\text{OCH}_3)_3$ results in B_2O_3 , and SiH_4/NH_3 mixtures lead to amorphous Si_3N_4 . Also the deposition of amorphous Al_2O_3 layers with high dielectric strength from $\text{Al}_2\text{Cl}_6/\text{O}_2$ mixtures in glow discharges has been reported. Such systems also provide examples of the formation of amorphous layers by chemical vapour deposition.

2.1.3.4 Chemical Vapour Deposition

Chemical vapour deposition (CVD) depends on spontaneous reactions taking place between different gases, or between a gas and the wall of the vessel. These methods are of growing interest in the context of monocrystal growth (gas phase epitaxy), but they also permit the preparation of amorphous substances. The best known method in this area is the production of high-purity SiO_2 by hydrolysis of SiCl_4 in an oxyhydrogen flame, together with SiCl_4/O_2 pyrolysis. It leads to

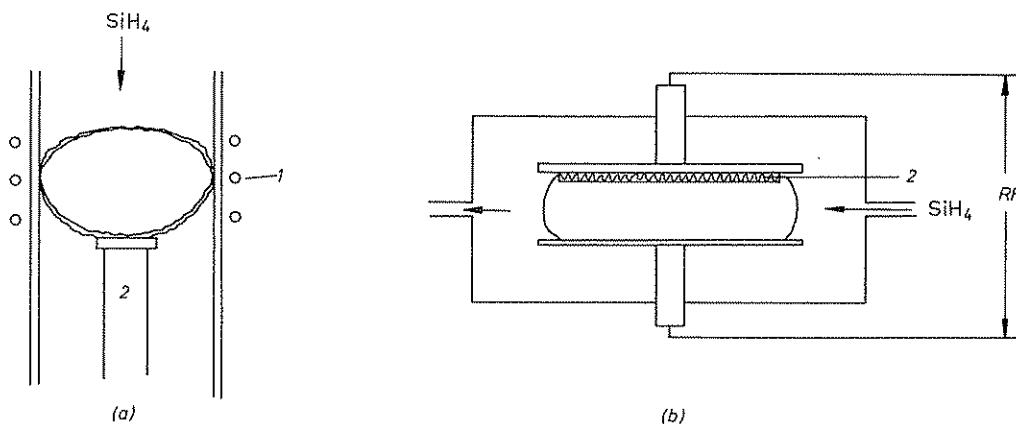


Fig. 2.9. Deposition of amorphous layers by decomposition of suitable gases or gas mixtures, such as

SiH_4 , in a glow discharge, with (a) inductive and (b) capacitive energy supply.

(1) induction coil; (2) substrate holder with temperature control.

deposition of low-water, high-purity vitreous silica forms as needed in fibre optics.

2.1.4 Transformation of Crystalline Solids to the Amorphous State

Non-thermal transformation of crystalline solids to forms of the amorphous state requires the application of sufficiently strong external forces. For example, atoms can be excited by pulse transmission to leave their positions of equilibrium. Vitreous states of minerals with a high SiO_2 content can result from impact by extraterrestrial bodies. This may explain the existence of lunar glasses or tectites in certain regions of the earth's surface [2.457, 2.458]. Under certain conditions, solid-state reactions are accompanied by the structural disintegration of the parent materials, without the development of crystalline ordering in the resulting product. Amorphous substances can thus be obtained, at least as intermediate states. Examples are the thermal dehydration of kaolinite, and the preparation of amorphous $\text{KFe}_3\text{O}_3(\text{SO}_4)_2$ by heating jarosite, $\text{KFe}_3(\text{OH})_6(\text{SO}_4)_2$, to approximately 500 K.

2.1.4.1 Amorphous Solids Formed by Mechanical Processing

The mechanical amorphization of quartz by vibratory grinding has been reported by Schrader and co-workers [2.431] following comprehensive investigations. The ESR spectra indicated a high density of broken bonds, and the associated increase in chemical reactivity was studied [2.432, 2.433]. Intense grinding of kaolin converts it to the amorphous state [2.434], and also the modification of the setting behaviour of cement by intense mechanical activation has been described [2.436].

High densities of defects, which can lead to amorphization of structures in regions close to the surface, must indeed be considered whenever solids are exposed to mechanical stresses. The formation of a largely disordered Beilby layer during mechanical polishing or run-in of bearings or gear profiles is quite likely in view of the high local energy density. The associated phenomena are aspects of tribochemistry, a discipline of major technological importance [2.436].

2.1.4.2 Amorphous Solids Formed by Irradiation

Irradiation with fast neutrons or the impact of highly accelerated ions can eliminate the lattice periodicity of crystalline solids, without the need to pass through an isotropic melting phase.

The density of quartz, for example, is reduced by 15% to a minimum of 2.26 g cm^{-3} by the effect of 1.5×10^{20} neutrons per cubic centimetre. The refractive index is 1.467. Similar values are obtainable with tridymite or cristobalite [2.54, 2.55]. The solid thus obtained is amorphous and isotropic, and its properties differ little from those of vitreous silica. The latter has a density of 2.205 g cm^{-3} and a refractive index of 1.457. Studies have shown that the short-range order is comparable [2.56]. A further increase in density during subsequent thermal treatment has been observed in cases of low irradiation doses. This was accompanied by recrystallization to α -quartz. High irradiation doses, on the other hand, led to the formation of vitreous silica during subsequent heat treatment at 1373 K, which means that the density decreases further. Beryl, $\text{Be}_2\text{Al}_3\text{Si}_6\text{O}_{18}$, was transformed into the vitreous state in the same way.

The depth of penetration of charged particles is limited to regions near the surface. Amorphous Ge layers with a thickness of 60 nm are obtained, for example, by bombarding Ge monocrystals with oxygen ions accele-

vated to 10^5 eV , using a dose of 10^{15} ions per square centimetre [2.57].

2.1.4.3 Generation of Amorphous States by Shock Waves

Experiments by De Carli and Jamieson [2.58] have shown that quartz monocrystals can be transformed to the amorphous state in certain regions even by shock waves of no more than 360 kbar and a maximum front temperature of 873 K. The product thus obtained, with a density of 2.22 g cm^{-3} and a refractive index of 1.46, is very similar to vitreous silica. Pulse transmission is through metal plates driven by an explosion wave. The result is remarkable, since the shock is applied for only 10^{-5} s . The melting point of α -quartz is about 1673 K, but owing to the high viscosity the linear melting rate at this temperature is only about $10^{-8} \text{ cm min}^{-1}$ [2.59]. Consequently, a conventional melting mechanism is out of the question. It should be added that the density of amorphous SiO_2 obtained from a shock wave of 600 kbar is almost identical to that of the product obtained from experiments with 360 kbar. The amorphous state is similar to that of vitreous silica, and in these experiments it is found to coexist with the still unchanged crystalline regions of the quartz sample, so that it can be defined as an SiO_2 modification in the context of thermodynamics (see Section 3.2.2.1). Structural features which characterize the amorphous SiO_2 obtained by shock compression have been described by Mashimo and co-workers [2.438].

2.1.4.4 Reactions of Crystalline Solids with Formation of Glasses

The oxidative treatment of the surface of Si monocrystals in a stream of oxygen or water vapour at high temperature has been thoroughly studied and found to be of practical interest. Kinetic studies of the growth of the amorphous SiO_2 layer indicated a diffusion-

limited reaction between the Si monocrystal surface and O_2 or H_2O . The reaction rates for O_2 and H_2O in vitreous silica were approximately equal to the values found by other methods [2.60]. Such surface layers can be applied in a plasma, e.g., of oxygen, at much lower temperatures and thus under relatively non-invasive conditions [2.50].

2.2 Thermodynamic Description of the Glassy State

Glasses are related to isotropic liquids or melts, and to vapours, as may be seen from the methods of their preparation explained in the previous chapter. Liquids can be interpreted both as condensed gases and, to some extent, also as highly disordered solids. It is, therefore, appropriate to refer to the theory of liquids for the description of the glassy state.

As far as the packing density is concerned, liquids are closer to solids, whereas with regard to the continuous displacements of atoms and subassemblies they appear closer to gases. Lattice or cell models are used, and consideration is given to the volume, also called free volume, which is usually larger than that of the crystal, with reference to the configurational statistics of free lattice points. These concepts can be traced back to Frenkel [2.62] and Eyring et al. [2.63], while Alfrey et al. [2.64] may have been the first to resort to the theory of the free volume in an attempt to explain glass formation.

Comparison with crystals should be more valid, at least in small regions, at temperatures close to the solidification point or to supercooling. A continual interchange of sites occurs, resulting in instability of shape. Gutzow and co-workers [2.65] constructed a model to describe processes of association, which lead to enlargement of structural regions. As the

temperature is raised further, the structure of liquids comes closer to that of gases, and at a critical temperature liquids undergo a continuous transformation into the vapour state. This temperature dependence can be expressed by a reduced version of van der Waals' equation, for example:

$$pV = RT + \left(b - \frac{a}{RT}\right)p \quad (2.4)$$

or in a more generalized version according to Clausius:

$$pV = RT + \frac{1}{3} \sum K(r_{ij})r_{ij} \quad (2.5)$$

The first term represents the kinetic energy, the second the interaction energy between atoms or subassemblies separated by r_{ij} . Equation (2.5) can be generalized further by introducing a radial distribution function [2.66]:

$$pV = RT - \frac{N_A}{6} \int_0^\infty \frac{d\varphi(r)}{dr} \varrho(r) 4\pi r^3 dr \quad (2.6)$$

This relationship expresses the significance of the distribution function $\varrho(r)$ and of the intermolecular potential $\varphi(r)$ [2.67].

The description of flow or transport processes also involves the relaxation time τ . This is the time interval required for the motion of an atom or group of atoms to adapt to the statistical mean value, e.g., by decaying to $1/e$ of the initial value. In other words, a statistically random motion that is independent of the initial state has been almost restored. This can be expressed according to Kirkwood [2.68] by the autocorrelation coefficient

$$z = K(t)K(t + \tau) \quad (2.7)$$

This specifies the mean scalar product of forces $F(t)$ acting at time t and the effect of these forces that still remains after the interval

τ . With $z = 0$, the particle will have no memory of the state of motion that existed at time t .

Statistical thermodynamic calculations on this basis have so far been possible only for the simplest systems, such as inert gas systems consisting of some hundreds of atoms [2.69]. However, relaxation times of $\tau > 10^{-8}$ s are too great to be analyzed in this way, so that macroscopic phenomenological descriptions of the liquid state have been necessary in all cases of practical relevance.

2.2.1 Relaxation Behaviour in Liquid and Vitreous States

The fundamental relations are introduced by the example of mechanical relaxation. Although implicitly contained in the effects initiated by compressive and tensile stresses, structural relaxation will, for completeness, be treated in connection with thermal relaxation. This will be followed by a discussion of the temperature dependence of the viscosity and of various models for describing the observed phenomena. Finally, brief reference will be made to the method of correlation spectroscopy.

2.2.1.1 Mechanical Relaxation

Glasses, being solids, undergo elastic deformation in response to the action of external forces. For example, angular deformation, as shown in Fig. 2.10, may occur as a result of a shear stress $S_G = F/A$.

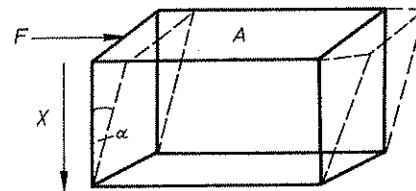


Fig. 2.10. Torsion (shear) of a solid exposed to action of tangential stress $S_G = F/A$.

The stress applied to the vitreous body is assumed to be within the elastic limit, so that its original state will be restored after relieving the stress. The deformation depends on the torsion or shear modulus G and is given by the relationship $\alpha = (1/G)S_G$. G is related to the tensile modulus $E = (l/\Delta l)S_E$ and the adiabatic compressibility κ by the relationship

$$E = 2G(1 + \mu) \quad \kappa = 3(1 - 2\mu)/E \quad (2.8 a)$$

S_E corresponds to a tensile or compressive stress acting in the direction of the normal. μ stands for Poisson's ratio of transverse contraction, $\mu = (\Delta d/d)/(\Delta l/l)$, and can be determined, for example, by measuring the velocities of longitudinal and transverse propagation v_l and v_{tr} of sound waves in a relatively simple way:

$$\mu = 0.5 \left[1 - \frac{v_{tr}^2}{v_l^2 - v_{tr}^2} \right] \quad (2.8 b)$$

G can be obtained from the density ϱ and the transverse sound propagation velocity according to $G = \varrho v_{tr}^2$.

Consideration of the time dependence of the elastic stress leads to

$$\frac{d\alpha}{dt} = \frac{1}{G} \frac{dS_G}{dt} \quad (\text{Hookean body}) \quad (2.9)$$

In cases of plastic deformation of the vitreous body, i.e., with the onset of viscous flow, the shear stress S_G will be proportional to the gradient in the direction x of the relative velocity of successive layers (Fig. 2.10). The constant of proportionality is the dynamic viscosity η :

$$\frac{dv}{dx} = \frac{S_G}{\eta} \quad (\text{Newtonian liquid}) \quad (2.10)$$

The combination of Equations (2.9) and (2.10) with a deformation rate $d\vartheta/dt$ results in Maxwell's differential equation for viscoelas-

tic flow behaviour:

$$\frac{d\vartheta}{dt} = \frac{1}{G} \frac{dS_G}{dt} + \frac{S_G}{\eta}, \quad \text{or} \quad \frac{dS_G}{dt} = G \frac{d\vartheta}{dt} - \frac{S_G}{\eta/G} \quad (2.11)$$

The rate of variation of the shear stress with time (dS_G/dt) is proportional to the rate of deformation ($d\vartheta/dt$). If flow processes are involved, the shear stress caused by deformation will be smaller, the greater S_G and the smaller the quotient η/G . The latter represents a relaxation time describing the rate at which the body escapes the external influence by the decay of the shear stress.

$$\eta = G\tau \quad \eta = \frac{3}{5\kappa}\tau \quad (\text{for } \mu = 0.25) \quad (2.12)$$

Constant deformation ($d\vartheta/dt = 0$) leads to

$$\frac{dS_G}{dt} = -\frac{S_G}{\tau}, \quad S_G = S_G' \exp(-t/\tau) \quad (2.13)$$

which means $S_G = S_G'/e$ for $t = \tau$. Equation (2.10) will again result from Equation (2.11) if the deformation rate $d\vartheta/dt$ is kept constant, so that this will be a case of stationary flow of a Newtonian liquid.

Thus, according to Equation (2.11), whether the substance in question is to be regarded as a glass or a supercooled liquid depends on the duration of the observations. The term S_G/τ can be neglected if the observation time $\Delta t \ll \tau$, because the body is actually Hookean. If a body strikes a liquid, such as water, with sufficient velocity, the effect can be compared to bouncing on concrete, even if the influence of surface tension is neglected. In the opposite case, i.e., $\Delta t \gg \tau$, glasses and even crystalline solids can undergo plastic deformation.

The scriptural text from Deborah's song "... the mountains melted from before the Lord ..." (Book of Judges, Chapter 5, Verse 5) has been interpreted in the sense that only a divine being could have the time needed to

oversee such long-term changes. Consequently, a "Deborah number" DN has been defined as the ratio of the relaxation time τ to the observation time Δt [2.70]. Melts or liquids in the region of $DN \gg 1$ have the properties of solids, and thus should be regarded as glasses, whereas the stability of shape ceases to exist with $DN \ll 1$. The intermediate region, i.e., the glass transition, is characterized by a Deborah number close to 1. Efforts have been made recently to express the same condition by means of the Lillie number $L_1 = d\tau/dt = (-dB\tau/dt)$, with $B = -dT/dt$ (cooling rate) [2.459].

Douglas [2.71] uses this viewpoint for a definition of the glassy state:

"A glass is a liquid with a relaxation time that is no longer observable."

Kauzmann [2.72] formulates this more precisely:

"In the glass state, the relaxation time of some degrees of freedom is long, as compared to the duration of the experiment. Consequently, the glass transition temperature should largely depend on the type of property determined experimentally, on the duration of the experiment, and on what we mean by long time."

Some questions have not yet been answered: what should be understood as "no longer observable", which method of measurement is used, how long is shear stress, for example, allowed to act, and how accurately can one measure the initial deformation or the decay of the applied stress?

A common measuring principle is based on applying a periodic stress to the glass body to be investigated, so that $\mathcal{J} = \mathcal{J}_0 \cos \omega t$. For example, one can measure the attenuation of vibrations of a torsional pendulum, or resonance arrangements are used to determine the logarithmic decrement λ , from which the relaxation time τ can easily be calculated using

the equation

$$\lambda = \pi/\omega\tau \quad (2.14)$$

If the torsional modulus G or the compressibility κ is known, the viscosity can also be calculated according to Equation (2.12).

Evaluation in the complex plane is a common method. S_G , G and \mathcal{J} in Equation (2.11) must then be replaced by the complex quantities S_G^* , G^* , and \mathcal{J}^* . The differential equation can be solved from the relationships

$$S_G^* = G^* \cdot \mathcal{J}^* \quad \text{and} \quad (2.15)$$

$$G^* = \frac{\omega\tau}{\omega\tau - i} G \quad \text{also using} \quad \mathcal{J}^* = \mathcal{J}_0 e^{i\omega t}$$

Separation into real and imaginary parts results in

$$G^* = G' + iG'' = \frac{\omega^2\tau^2}{1 + \omega^2\tau^2} G + i \frac{\omega\tau}{1 + \omega^2\tau^2} G \quad (2.16)$$

so that the loss factor is

$$\tan \delta = \frac{G''}{G'} \quad (2.17)$$

$\tan \delta = \lambda/\pi$ is also called the "internal friction", which must not be confused with the coefficient of internal friction, i.e., the viscosity η .

The measurement of λ or $\tan \delta$ gives the relationship between the relaxation time τ and frequency ω , so that the functions G'/G and G''/G can be calculated according to Equation (2.16). Plotting these as functions of $\log \omega\tau$ leads in the former case to a rising S-shaped curve with inflection point at $\omega\tau = 1$ and $G'/G = 1/2$, and in the latter to a bell-shaped curve with a maximum of $G''/G = 1/2$ at $\omega\tau = 1$. This means that an inflection point or an extreme value in the curves is not observed unless the measuring frequency passes through

a "flow process" characterized by the relaxation time τ . With a frequency of 10^{-1} Hz, this condition is met by a relaxation time of 1.6 s, which, with a typical value of, for example, 6.24 GPa for As_2S_3 , leads to a viscosity of $\eta = 10^{11}$ dPa s.

Measurements are carried out at various frequencies, and the temperature is also varied, so that the internal friction can be covered in a wide range of different relaxation times. It was found that glasses in general do not behave like simple Maxwellian bodies. For example, high shear stresses were accompanied by lower viscosities [2.73], whereas with a very low shear velocity of 10^{-8} cm s $^{-1}$ an induction time was observed [2.74]. Hence, the viscoelastic behaviour is not strictly linear, which means that additional non-linear terms must be introduced into Equation (2.13). This fact can be interpreted as meaning that the internal friction of glasses and their melts has to be described by a distribution of relaxation times [2.75, 2.76], the latter changing with temperature. De Bast and Gilard [2.76] introduced the expression

$$S_G = S_G^c \exp\left(-\frac{t}{\tau}\right)^b \quad (2.18)$$

to replace (2.13). Here b tends to 1 in the region of $(t/\tau) \geq 100$, which means that a simple Maxwellian body is involved. However, the value of b is about 0.5 at viscosities of 10^{15} dPa s [2.77, 2.78]. b is about 1/3 for $10^{-3} < (t/\tau) < 10^{-4}$. The curves of G'/G and G''/G as functions of $\log \omega\tau$ are progressively flattened with decreasing values of b , and with $b = 0.1$ the inflection point in the former case and the maximum in the latter have practically disappeared [2.79]. Against the background of the melt, the relaxation time behaviour can be described almost correctly in terms of a thermodynamic interpretation of τ up to the glass transition temperature ($\eta = 10^{13}$ to 10^{15} dPa s). Considerations based on the autocorrela-

tion coefficient [2.7] seem to be useful only within these limits.

The temperature dependence of the measured relaxation time is influenced by different relaxation processes in different temperature regions, so that the Arrhenius equation

$$\tau = \tau_0 \exp [E_\eta/RT] \quad (2.19)$$

usually applied to describe the temperature dependence of reaction processes, will at best be valid only within narrow temperature limits.

Particular experimental requirements have to be met for measurement of mechanical relaxation above the glass transition temperature, as the specimen then starts to become deformed by the gravitational field. Ultrasound measurement [2.80] is one possible method. Corsaro [2.81] has reported on an acoustic dilatometer. Viscosity measurements are often simpler for practical purposes. The relaxation time can then be calculated using Equation (2.12). The specimen must appear as an elastic solid in the transition range with measuring frequencies of $\nu > 10^{-2}$ Hz. Flow processes or site interchanges are virtually absent in pure glass-forming compounds under such conditions, so that corresponding effects can hardly be expected. It has been shown, however, that damping effects can be caused even by traces of impurities, such as OH groups or alkaline oxides in vitreous silica, far below the glass transition temperature. Accordingly, even special glasses of complex composition are characterized by a temperature-dependent spectrum of internal friction, which has been interpreted in terms of structural chemistry in a great number of papers. The structural skeleton of glass is rigid, and the behaviour of the sample is largely that of a Hookean body. Nevertheless, local processes of site interchange occur within the structure. This occurs, for example, when alkalimetal ions move between different positions which are separated by potential barriers

(see Section 4.1.1), and obviously an interchange between bridging Oxygens and terminal oxide ions must be taken into consideration [2.82]. E_η in Equation (2.19) must be replaced in such cases by the activation energy of the relevant process. Bartenev and co-workers [2.439] have recently reported on relaxation mechanisms that occur below the glass transition temperature T_G .

Mechanical relaxation of glass was reported in early work by Rötger [2.83] and in more recent publications, mainly by Stevels and coworkers [2.84], Day and co-workers [2.85], and by Tayler and Rindone [2.86]. A thorough study of the viscoelastic flow behaviour in the region of T_G has been described by Perez and co-workers [2.448], who used a low-frequency torsional pendulum for measurement. Phenomena of the same kind have also been found in metallic glasses [2.87].

2.2.1.2 Thermal and Structural Relaxation Processes

Structural relaxation, as observed in the glass transition region, relates to the time dependence of macroscopic properties following rapid changes of temperature and/or pressure. Its general features are reported in several recent papers [2.478, 479, 480]. Rekhson [2.493] has given a review on the viscoelasticity of glass, and Mazurin has reported on mechanical relaxation in inorganic glasses [2.494].

If a glass melt is cooled, a thermal equilibrium still exists in the region of supercooling. We may assume that initially the redistribution of internal energy or enthalpy between the degrees of freedom of the system is able to keep pace with the cooling rate $q = dT/dt$. The number and type of ruptured bonds and thus the size of flow units as well as their translational, vibrational, and rotational behaviour are subject to change with the temperature. Consequently, temperature change is accom-

panied by structural changes in the melt. The term "structural relaxation" adequately describes this process.

Delays are observed if the reaction rate, which is limited by such processes whereby the system approaches a new equilibrium state with every infinitesimal decrease in temperature, falls behind the cooling rate. The system can then no longer keep pace with the cooling rate. The amount of enthalpy remaining in the melt is greater than that expected for thermodynamic equilibrium at that temperature. Consequently, the supercooled melt becomes metastable with regard to the crystalline state (Fig. 2.11). The structural relaxation process freezes in the transition range. The supercooled melt thus changes to the vitreous state; therefore, glasses are also metastable with respect to the supercooled melt, and are thus metastable in a dual sense. Glasses are said to be in the frozen state of a supercooled melt.

Following studies by Simon [2.89], who compared glass formation to a freezing process, Haase [2.88] proposed the following definition of the glassy state:

"A frozen supercooled liquid is to be regarded as a glass."

Irrespective of the mode of production, non-crystalline solids below the glass transition temperature can be regarded

"as a kinetically frozen thermodynamic system"

according to Gutzow [2.152]. Recently, Cooper [2.481] enlarged the definition to include all processes by which a random structural element is "frozen in".

This process can be described by a differential equation analogous to Equation (2.11):

$$\frac{d\Delta H}{dt} = C_p \frac{dT}{dt} - \frac{\Delta H}{\tau} \quad (2.20)$$

If the cooling curve is subdivided into a succession of infinitesimally small intervals, one can regard, T as constant within any interval, and thus $(dT/dt) = 0$; thus, each of these infinitesimal partial regions follows the equation

$$\frac{d\Delta H}{dt} = - \frac{\Delta H}{\tau} \quad (2.21)$$

The temperature dependence of τ should be expressed, within certain limits, by Equation (2.19), or by some other suitably modified relationship (cf. Section 2.2.1.3).

The relaxation time increases with falling temperature, and the freezing process at different temperatures has been found to depend on the cooling rate applied. The faster the cooling rate, the higher the temperature of the transition region for the glass concerned (Fig. 2.11).

Consequently, glasses with different thermal histories show differences in their structures, even though they have the same composition. Different structural configurations for certain temperatures are spatially fixed as functions of this thermal history. According to Tool [2.90], one can define a fictitious temperature at which the structure of a liquid becomes fixed. Alternatively, one can define an internal order parameter, as Davies and Jones [2.91] have done. Hence, the description of the vitreous state requires not only the specification of variables of state, such as pressure and temperature, but the addition of at least one more parameter. The hysteresis that results from a cycle of cooling and heating with the same rate in each direction (Fig. 2.11) expresses the relaxation process whereby the supercooled melt changes to the vitreous state and, vice-versa, the non-equilibrium system of the glass reverts to the equilibrium state of the melt.

The heat capacity curve, too, is shown in Fig. 2.11. According to Moynihan and co-workers [2.92], $H = H(T, t)$ and the equation

$$\frac{dH}{dt} = \left(\frac{\partial H}{\partial t}\right)_T + \left(\frac{\partial H}{\partial T}\right)_T \left(\frac{\partial T}{\partial t}\right) \quad (2.22)$$

can be used together with Equations (2.19 and 2.21) in the case of $(\partial H/\partial t)_{T=T_G}$ to express the difference between the observed heat capacity $(dH/dT) = C_p$ and the heat capacity of glass $(\partial H/dT)_t = C_{p,G}$ in the following way:

$$C_p - C_{p,G} = \mp \frac{\Delta H_{T_G}}{|q| \tau_0 \tau_G} \exp[-E_\eta/RT_G] \quad (2.23)$$

(-) heating, (+) cooling

On the assumption that the dependence of $(C_p - C_{p,G})$ and ΔH_{T_G} on the heating or cooling rate q is nearly negligible (compare Fig. 2.11), a function relationship between q and T_G can be specified as follows:

$$\frac{d \ln |q|}{d(1/T_G)} \approx - \frac{E_\eta}{R}, \quad q = q_0 \exp[-E_\eta/RT_G] \quad (2.24)$$

This relationship corresponds to Bartenev's equation [2.93, 2.94] and has been confirmed in numerous experimental studies. Plotting $\ln |q|$ against $1/T$ leads to straight lines, whose slopes can be used to determine the activation energy of viscous flow in the glass transition region. The results are in good agreement with the values found by other methods for As_2Se_3 [2.92, 2.95], B_2O_3 , and other glasses [2.92]. A review of these studies has been published by Mazurin [2.79].

The effects of structural relaxation of glass melts and glasses are also seen in other properties, such as the density, molar volume, or molar refractivity. For example, results obtained by Macedo and Napolitano [2.96] for B_2O_3 glass are shown in Figure 2.12. The sample, which is initially in equilibrium at 583.5 K, i.e., above the T_G value, has a refractive index $n_D = 1.45337$, measured at 298 K. Subsequent heating to temperatures below

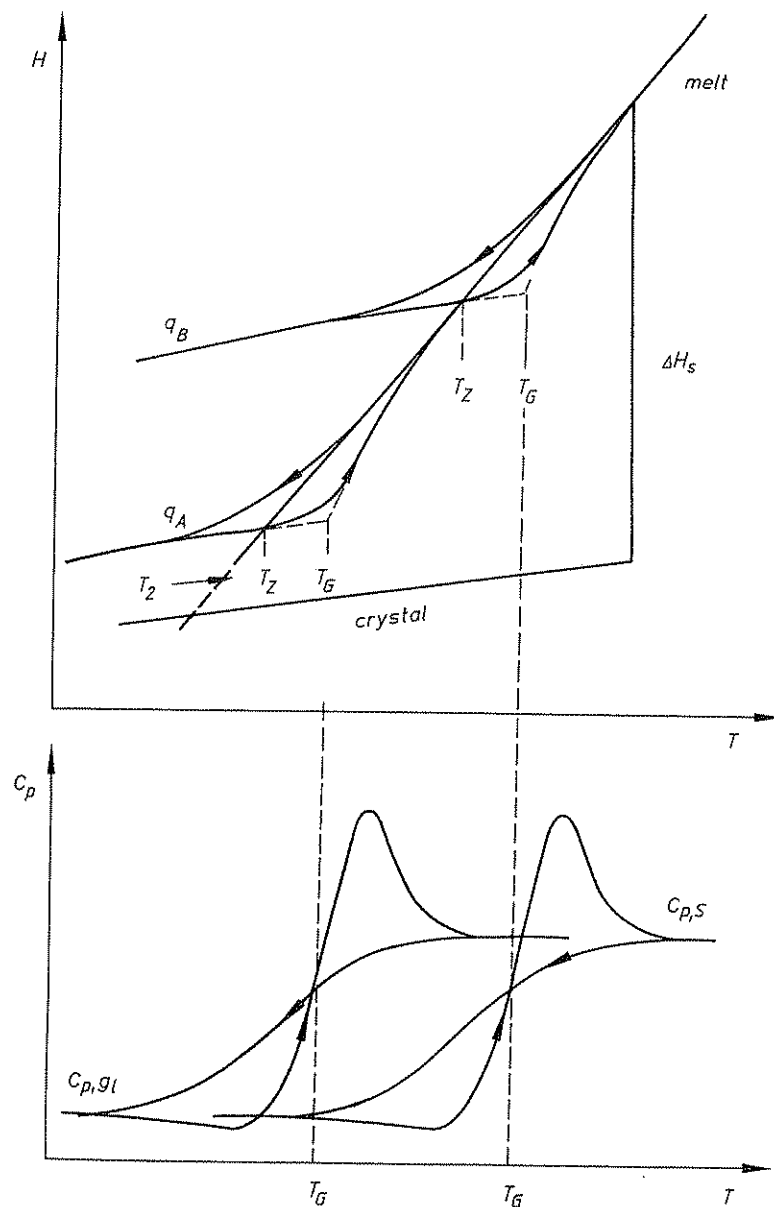


Fig. 2.11. Temperature dependence of enthalpy H and heat capacity C_p in the transition from the melt to the vitreous state and vice-versa.

Cooling and heating rates $q_B >$ cooling and heating rates q_A , $T_G =$ transition temperature, $T_Z =$ freezing temperature; for T_Z see Section 2.2.3.1.

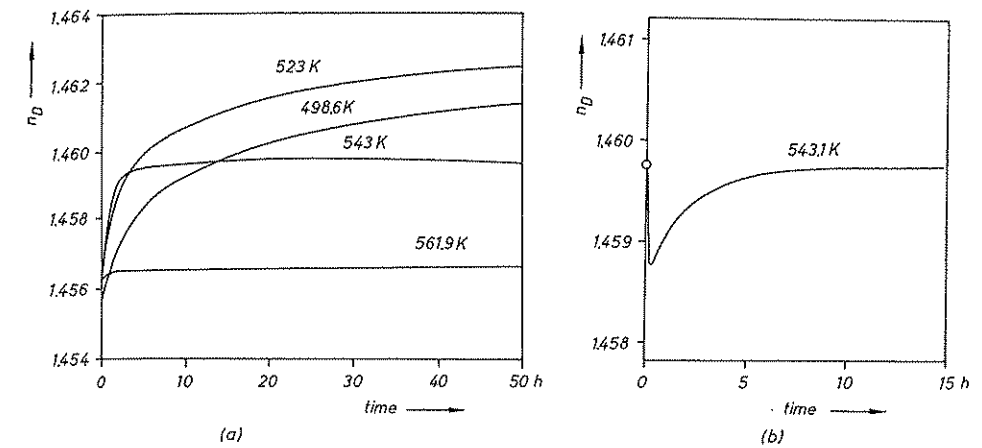


Fig. 2.12. Time dependence of the refractive index of B_2O_3 glass as measured at 298 K after quenching from 583.5 K and subsequent annealing at the temperatures

shown (a), and refractive index curve (at 298 K) of a sample kept at 498.6 K for 14 hours, during heating to 543 K (b), according to [2.96].

583.5 K and quenching to room temperature gave the curves shown. The higher the holding temperature, the lower the optical densification, according to expectation, and the faster the adjustment to the new final value ("cross-over experiments", Figure 2.12 a). If, for instance, the sample is heated to 543 K, after holding for 14 hours at 498.6 K, the value of $n_D = 1.4597$ throughout at 298 K will by no means remain unchanged. It shows an initial decrease, and only then the adjustment to the refractive index that is characteristic of 543 K (see Fig. 2.12 b). It necessarily follows that in this case at least two relaxation processes must be postulated to describe the temperature-time behaviour of the glass, namely a rapid process associated with the temperature change, and a slower reaction which obviously corresponds to the structural relaxation. The phenomena of glass annealing are described in a review paper by Narayanaswamy [2.496].

Such relationships are very important for practical applications, in view of the very narrow tolerances for the refractive index of optical glasses [2.97].

Arndt et al. [2.482] studied the anomalous

behaviour of the refractive index during the annealing of densified, amorphous SiO_2 . The sample had been densified plastically by up to 16 %, then isochronically annealed at 600 and 800 °C. The isothermal annealing was found to change the density monotonically, but the stretched exponential form frequently observed in the relaxation of complex systems was not found in this case. It was suggested that this may be due to structural rearrangements during the annealing process, which do not follow the same path as those occurring in the densification process.

Moynihan et al. [2.483] have proposed a model for nonlinear structural relaxation, and Rekhson [2.484] has recently given a review of memory effects in glass, whereby the processes that occur during the glass transition are affected by the thermal history.

2.2.1.3 Temperature Dependence of Viscosity

By combining Equations (2.19) and (2.12) we obtain the relationship